Identifying Magnetic Anisotropy of the Topological Surface State of $Cr_{0.05}Sb_{1.95}Te_3$ with Spin-Polarized STM

Fang Yang, Y. R. Song, H. Li, K. F. Zhang, X. Yao, Canhua Liu, Dong Qian, C. L. Gao,* and Jin-Feng Jia†

Department of Physics and Astronomy, Key Laboratory of Artificial Structures and Quantum Control (Ministry of Education). Shanghai Jiao Tong University, Shanghai 200240, China

(Received 2 April 2013; revised manuscript received 24 May 2013; published 25 October 2013)

The surface magnetic property plays a key role in determining magnetic related quantum phenomena of magnetic topological insulators. Using spin-polarized scanning tunneling microscopy, we investigate the surface magnetism and anisotropy of a Cr doped topological insulator: $Cr_{0.05}Sb_{1.95}Te_3$. It is found that the topological surface state of $Cr_{0.05}Sb_{1.95}Te_3$ is spin polarized in the surface plane while the bulk shows a ferromagnetism with an out-of-plane easy axis. The upper and lower branch of the helical Dirac cone harbors the opposite spin polarization and the polarization at the Dirac point is zero. Our results show the complexity of surface magnetism of magnetic doped topological insulators.

DOI: 10.1103/PhysRevLett.111.176802 PACS numbers: 73.20.-r, 75.30.Gw, 75.70.Rf

The discovery of three-dimensional topological insulators (TIs) [1,2] opens a new category of quantum systems characterized by a gapless spin-momentum locked Dirac-like surface state in the bulk band gap protected by time reversal symmetry. Relying on the proper manipulation of the topological surface state (TSS), a lot of novel quantum phenomena have been theoretically proposed such as a magnetic monopole [3], Majorana fermions [4,5], and the quantum anomalous Hall effect (QAHE) [6]. As a key to realizing the QAHE, special attention has been paid to the coupling of the TSS with the perpendicular magnetic field, which eventually breaks the time reversal symmetry and opens a gap at the Dirac point [7]. An intuitive attempt was made to grow a magnetic adlayer on the surface of TIs [8–10]. Very contradictory results, however, have been reported concerning the gap opening at the Dirac point even in the very same system of a Fe adlayer on Bi_2Se_3 [11,12]. Further study shows that the magnetic moments of Fe are in-plane favored under a 1% monolayer of Fe on Bi_2Se_3 [13]. The effect of the magnetic adlayer on the TSS is still under debate. Alternatively, it was found that perpendicular bulk ferromagnetism can be obtained by doping the TI with magnetic ions such as Cr, Fe, V, etc. [14–17]. A gap opening as large as tens of milli–electron volts [18] was observed by angle resolved photoemission spectroscopy in the Fe doped Bi_2Se_3 even in the absence of bulk ferromagnetism. A proposed explanation is that a three-dimensional TI doped with magnetic impurities in the bulk can have a regime where the surface is magnetically ordered but the bulk is not [19]. A recent spin resolved angle resolved photoemission spectroscopy measurement on Mn doped Bi_2Se_3 [20] shows the opposite perpendicular spin polarization on the upper and lower band of the gap-like feature, while surprisingly the bulk is in-plane ordered [21] indicating that the magnetic anisotropy of the TSS is not necessarily coherent with that of the bulk. It is clear that the magnetic anisotropy of the TSS determines the behavior of the TSS (an out-of-plane spin polarization opens the gap while the in-plane one doesn't). Thus, when speaking of the surface magnetism of a magnetic doped TI, it is important to clarify the magnetism of the TSS and the bulk.

In this Letter, we took advantage of spin-polarized scanning tunneling microscopy (SPSTM) operating in a vectorial magnetic field and investigated the surface magnetic properties (especially anisotropy) of $Cr_{0.05}Sb_{1.95}Te_3$. It was found, despite the well defined out-of-plane magnetic easy axis of the bulk, that the TSS showed an in-plane ferromagnetism with an opposite spin polarization below and above the Dirac point. Our results indicate that the magnetic anisotropy of the TSS does not simply inherit that of the bulk at the surface and the TSS plays an important role in determining its own easy axis.

Single crystals of $Cr_{0.05}Sb_{1.95}Te_3$ were grown by the modified Bridgman method [22]. $Cr_{0.05}Sb_{1.95}Te_3$ is particularly chosen because of its very high crystalline quality [22] and high Curie temperature ($T_c = 10$ K). It has a very well defined out-of-plane magnetic easy axis. $Cr_{0.05}Sb_{1.95}Te_3$ single crystals were cleaved in ultrahigh vacuum ($< 1 \times 10^{-10}$ mbar). The bulk magnetism of the crystal was measured with a vibrating sample magnetometer (VSM). SPSTM measurements were performed at 4.2 K in a vectorial magnetic field (in plane: 2 T; out of plane: 7 T) created by three sets of superconducting coils. The magnetic tip was prepared by coating antiferromagnetic Cr on tungsten tips. The magnetic direction of the tip can be roughly controlled by the Cr thickness, either in plane (> 30 nm) or out of plane (~ 5 nm) [23]. The tip spin polarization is carefully characterized in each measurement (see the Supplemental Material [24] for the characterization of the tip orientation). SPSTM was operated in the spectroscopy mode using the lock-in technique with a 10 mV modulation at 985 Hz. The obtained dI/dV curve depends on the relative magnetic orientation between the

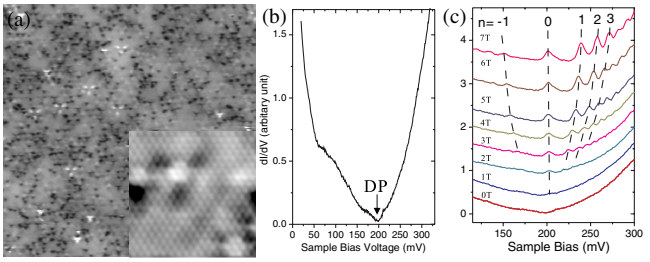

FIG. 1 (color online). (a) STM topographic image of cleaved $Cr_{0.05}Sb_{1.95}Te_3$ surface ($V = 520$ mV, $I = 200$ pA, 80 nm $\times$ 80 nm). The inset shows the atomic resolution image ($V = 450$ mV, $I = 200$ pA, 10.6 nm $\times$ 10.6 nm). (b) Typical tunneling spectrum on the surface around the energy of the band gap. (c) dI/dV curves in different magnetic fields (0–7 T) showing the Landau levels of the topological surface state.

sample and tip. A detailed description of the technique can be found elsewhere [25].

Figure 1(a) gives the morphology of the cleaved surface, which is flat and atomically ordered (see the inset). The image shows bright protrusions and dark intrusions, which are the variation of the local density of states (LDOS) due to Cr dopants or Sb-Te substitutions [22,26]. The presence of these defects, however, does not influence the TSS much. On arbitrary sites of the surface, scanning tunneling spectroscopy (STS) shows nearly identical dI/dV curves [see Fig. 1(b)], which have a minimum at ~210 meV above the Fermi level [27]. The Landau quantization of the Dirac cone structure was observed when applying an external magnetic field perpendicular to the surface agreeing with the one reported by Jiang *et al.* [26]. Figure 1(c) shows the dI/dV spectra in the magnetic field from 0 to 7 T. Discrete peaks start to appear at 1 T and more are visible as the field increases. The energy of these peaks obeys $|E_n - E_D| \propto \nu_F\sqrt{|n|B}$, where ν_F is the Fermi velocity, E_D is the Dirac point energy, and $n = 0, \pm1, \pm2\ldots$, consistent with the 2D character and linear dispersion of the TSS [1]. This demonstrates the persistence of the TSS in our Cr doped Sb_2Te_3. Furthermore, due to the fact that the $n = 0$ Landau level locates exactly at the Dirac point and does not move with the applied field in energy, the Dirac point can be precisely determined in this manner.

The magnetic properties of the surface were measured with both in-plane and out-of-plane spin sensitive tips. dI/dV curves of the same set (for example, a set of dI/dV curves to obtain the hysteresis loop) are taken at exactly the same location on the surface to avoid the influence of LDOS fluctuation. Although the dI/dV value may be different with different tunneling setpoints, the general shape of the dI/dV curves stays the same. Figure 2(a) gives the dI/dV spectra taken under the opposite perpendicular magnetic field ±3 T. The two curves are overlapping on each other near the Dirac point at 210 mV, but begin to deviate below 150 mV. The dI/dV curves are, however, totally the same if the external field is applied in the plane,

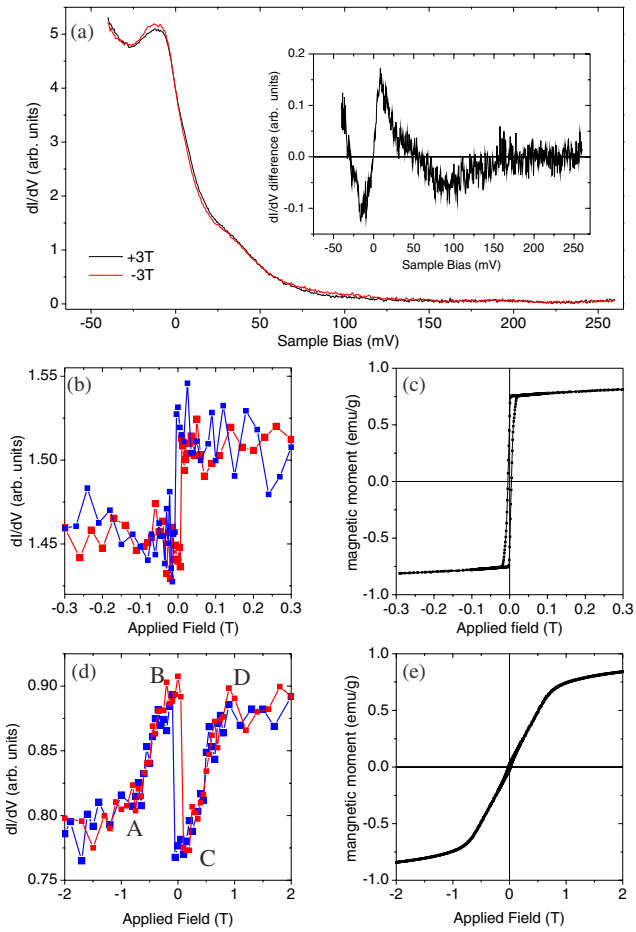

FIG. 2 (color online). (a) STS curves measured with an out-of-plane sensitive magnetic tip in the perpendicular field of +3 T (black) and −3 T (red). The inset shows the difference of these two curves. (b),[(d)] The hysteresis loop measured with an out-of-plane (in-plane) polarized Cr-coated W-tip on the surface through plotting the dI/dV value at $V = 25$ mV as a function of the magnetic field. (c),[(e)] Out-of-plane (in-plane) magnetic hysteresis loop of $Cr_{0.05}Sb_{1.95}Te_3$ measured with a VSM. See the Supplemental Material [24] for the low field details of (b) and (d).

which means the tip has a well defined out-of-plane spin sensitivity. The difference of the two curves is more clearly visible as plotted in the inset of Fig. 2(a). The difference is nonzero below 150 mV, while near the Dirac point, the difference is constantly zero. This means either there is no out-of-plane net spin polarization near the Dirac point or the spin signal is too weak due to the low LDOS (dI/dV value) in the bulk gap. This issue will be clarified in the further analysis of Fig. 3.

The surface magnetic hysteresis loop can be drawn by plotting the dI/dV value at a chosen energy of high spin polarization as a function of the applied field. Figure 2(b) shows the hysteresis loop measured with an out-of-plane sensitive tip. The square loop with a coercive force of 50 Gs is in perfect agreement with the bulk measurement

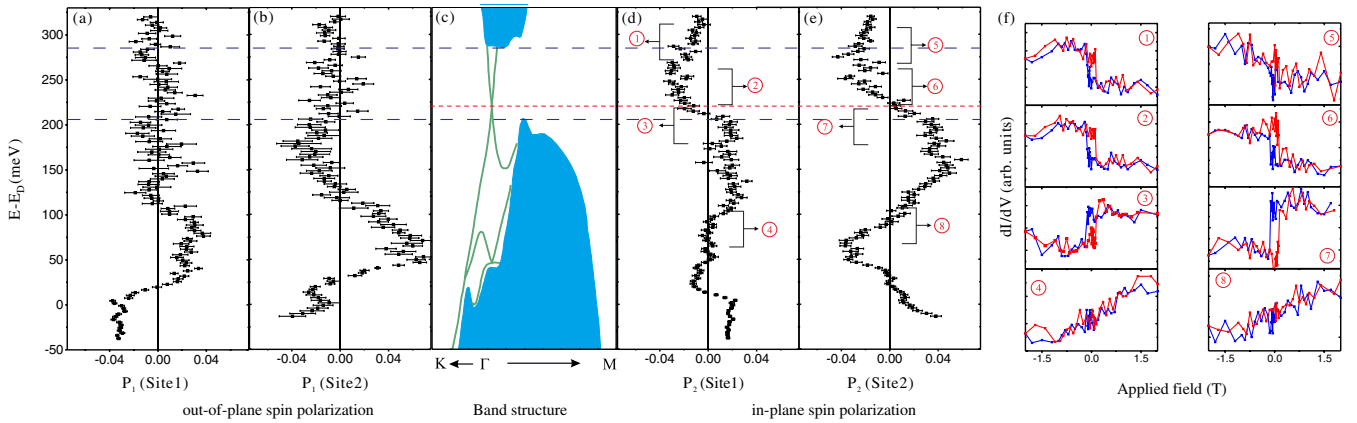

FIG. 3 (color online). (a,b)[(d,e)] show the out-of-plane (in-plane) spin polarization for two different sites on the surface calculated by formula 1(2) taken with the same in-plane polarized tip ($V_{\text{bias}} = 320$ mV, and $I = 275$ pA). (c) Calculated band structure extracted from Ref. [31]. (f) Hysteresis loops correspond to the energy in (d) and (e) as marked by 1–8, and the loops are integrated over the energy marked by brackets in (d) and (e). The red (blue) points indicate the increasing (decreasing) magnetic field. The dense (red) dashed line marks the energy position of the Dirac point, and the sparse (blue) dashed lines mark the up and down limits of band gap.

with the VSM at the same temperature of 4.2 K [see Fig. 2(c)]. It seems that the surface magnetism is simply the same as the bulk with a well defined out-of-plane easy axis. The situation, however, is not the case for the in-plane magnetism of the surface. Figure 2(d) gives the hysteresis loop measured with the in-plane sensitive tip at the same energy as Fig. 2(b). The loop is characterized by two distinguished features. One is marked by the smooth change of the dI/dV magnitude saturating at ± 1 T as marked by $A \leftrightarrow B$ and $C \leftrightarrow D$. The loop overlaps on each other when increasing (red curve) and decreasing (blue curve) the magnetic field. This feature is the same as the in-plane VSM results [see Fig. 2(e)]. When measuring perpendicular to the easy axis of a ferromagnet, the external field will drag the magnetic moment from the easy axis to the hard axis resulting in a hysteresis loop as shown Fig. 2(e) as one can expect. The feature of $A \leftrightarrow B$ and $C \leftrightarrow D$ characterizes the same contribution of the surface magnetism as in Fig. 2(b). Another feature is the square loop in $B \leftrightarrow C$ with a coercive field above 500 Gs, which is more than 10 times larger than the bulk coercivity. The square shape shows that this feature has an in-plane easy axis, which is not visible in the out-of-plane measurement due to its large saturation field. Since this pronounced feature has no correspondence in the bulk measurements [see Fig. 2(e)], it should originate purely from the surface. Thus, one can conclude that there are two different aspects of the surface magnetism: one is in plane and the other is out of plane. From the fact that the two features cause opposite changes in the dI/dV signal [see Fig. 2(d)], very probably they have different origins.

To reveal the origin of the out-of-plane and in-plane surface magnetism, the energy dependent spin polarization is plotted in Fig. 3 together with the calculated band structure of Sb_2Te_3 aligned by the Dirac point. In general, the spin polarization of the tunneling current in the SPSTM measurements is defined as the difference of two STS curves measured at opposite saturate fields divided by the sum of them [25]. In our case, with the clarification that $A \leftrightarrow B$ and $C \leftrightarrow D$ characterize the out-of-plane part of surface magnetism and $B \leftrightarrow C$ characterize the in-plane part, respectively, one can separate the out-of-plane and in-plane spin polarization from the single measurement with the in-plane sensitive tip by defining the out-of-plane part of spin polarization as

$$P_1 = \frac{G_A - G_B + G_C - G_D}{G_A + G_D}, \tag{1}$$

and the in-plane part as

$$P_2 = \frac{G_B - G_C}{G_B + G_C}, \tag{2}$$

where $G_i (i = A, B, C, D)$ is the differential conductance at the referred parts of the hysteresis loop as marked in Fig. 2(d) (see the Supplemental Material [24] for details of the definition). The resulting spin polarization as a function of the energy is plotted in Figs. 3(a), 3(b), 3(d), and 3(e). The out-of-plane [see Figs. 3(a) and 3(b)] and in-plane [see Figs. 3(d) and 3(e)] spin polarization are of the same order of magnitude. Here, the spin polarization of two different atomic sites (site 1 and site 2) are shown. It should be noted that although the surface LDOS is not homogenous due to the presence of doping and substituting, the measured spin polarization and hysteresis loops are very similar over all the surface area. Only the magnitude of the spin polarization slightly varies from site to site, which is reasonable due to the variation of the LDOS.

It can be seen from Fig. 3 that the out-of-plane spin polarization [see Figs. 3(a) and 3(b)] is zero in the bulk band gap and nonzero in the bulk bands. The in-plane spin polarization [see Figs. 3(d) and 3(e)], on the other hand, is

generally nonzero over the whole energy range investigated. Notice that the out-of-plane and in-plane spin polarization is obtained simultaneously with the same tip, which means the spin sensitivity is the same. This suggests that the Dirac states have no out-of-plane spin polarization, which is also supported in the out-of-plane measurement [see Fig. 2(a)]. In particular, the in-plane spin polarization crosses zero exactly at the Dirac point and shows the opposite spin polarization just above and below the Dirac point. The hysteresis loops plotted at these energies show opposite square shapes [loops 2, 3, 6, and 7 of Fig. 3(f)] which clearly reveal that the TSS has an in-plane magnetic easy axis. The nonzero in-plane spin polarization out of the band gap can be explained by the broad energy extension of the surface bands as can be seen in Fig. 3(c). In the energy farther above the Dirac point, loop 5 shows reduced in-plane easy-axis behavior and an inclined background due to the small out-of-plane part of the polarization. In particular, in the energy where the in-plane part vanishes, loops 4 and 8 [see Fig. 3(f)] clearly show a hard axis behavior. From the fact that the out-of-plane spin polarization is zero in the bulk band gap and the in-plane spin polarization changes its sign smoothly across the Dirac point, we can ambiguously draw the conclusion that the TSS is ferromagnetically ordered in the plane despite the coexistence of the out-of-plane ferromagnetism at the surface of $Cr_{0.05}Sb_{1.95}Te_3$ coming from the bulk bands.

The establishment of ferromagnetism in both bulk bands and the TSS in $Cr_{0.05}Sb_{1.95}Te_3$ is obviously raised by Cr doping. The main difference is the magnetic anisotropy. The magnetic anisotropy of the bulk is determined by the crystalline anisotropy, which is out of plane for the rhombohedron structure of Sb_2Te_3. The magnetic anisotropy of the TSS, on the other hand, is determined by various aspects [28,29]: the Rashba-Bychkov spin-orbit coupling favoring an in-plane easy axis, the hexagonal warping favoring an out-of-plane easy axis, and the coupling to the magnetic ions, in this case, the Cr-*d* electrons. The final magnetic easy axis is the result of the competition of these aspects. Our results show that $Cr_{0.05}Sb_{1.95}Te_3$ is an intriguing system possessing out-of-plane polarized bulk bands and an in-plane polarized TSS. Also, we resolve no gap opening at the Dirac point in STS because only the out-of-plane spin polarized TSS opens a noticeable gap at the Dirac point [29]. Very recently, the QAHE was reported in $Cr_{0.15}(Bi_{0.1}Sb_{0.9})_{1.85}Te_3$ [30] indicating the TSS may favor the out-of-plane magnetization with a gap opening. Comparing these two systems, the main difference is the doping level of Cr and the shift of the Fermi level by Bi substituting Sb. The different magnetic easy axis of the TSS of the two systems could be due to the different coupling strengths of the TSS to Cr-*d* electrons or the shift of the Fermi level, which changes the strength of the spin-orbit coupling or warping effect. All these clearly show the complexity of magnetism at the surface of magnetic doped topological insulators.

In conclusion, we have investigated the surface magnetic properties of ferromagnetically ordered $Cr_{0.05}Sb_{1.95}Te_3$ by SPSTM. It is demonstrated that the bulk bands possess an out-of-plane magnetic easy axis while the TSS is spin-polarized in the plane. The spin polarization is asymmetric with respect to the Dirac point. Our finding shows that much more attention should be paid to the surface magnetism of magnetic TIs. Due to the presence of the TSS, the surface magnetism does not simply inherit that of the bulk and may have its own characteristics. Surface related *ab initio* calculations are highly needed to further understand the physics of the TSS upon magnetic doping.

This work is supported by the National Basic Research Program of China (Grants No. 2012CB927401, No. 2011CB921902, No. 2011CB922200, and No. 2012CB821404), NSFC (Grants No. 11374206, No. 91021002, No. 11274228, No. 10904090, No. 11174199, and No. 11134008), the Shanghai Committee of Science and Technology, China (Grants No. 12JC1405300, No. 13QH1401500, No. 10JC1407100, No. 10PJ1405700, and No. 11PJ405200), and the Program for New Century Excellent Talents in University. D. Q. acknowledges additional supports from the Top-notch Young Talents Program and the Program for Professor of Special Appointment (Eastern Scholar) at Shanghai Institutions of Higher Learning. C. L. Gao acknowledges J. Henk and A. Ernst for helpful discussion.

*Corresponding author.
clgao@sjtu.edu.cn
†Corresponding author.
jfjia@sjtu.edu.cn

[1] M. Z. Hasan and C. L. Kane, Rev. Mod. Phys. **82**, 3045 (2010).
[2] X.-L. Qi and S.-C. Zhang, Rev. Mod. Phys. **83**, 1057 (2011).
[3] X.-L. Qi, R. Li, J. Zang, and S.-C. Zhang, Science **323**, 1184 (2009).
[4] L. Fu and C. L. Kane, Phys. Rev. Lett. **100**, 096407 (2008).
[5] M.-X. Wang, C. Liu, J.-P. Xu, F. Yang, L. Miao, M.-Y. Yao, C. L. Gao, C. Shen, X. Ma, X. Chen, Z.-A. Xu, Y. Liu, S.-C. Zhang, D. Qian, J.-F. Jia, and Q.-K. Xue, Science **336**, 52 (2012).
[6] R. Yu, W. Zhang, H.-J. Zhang, S.-C. Zhang, X. Dai, and Z. Fang, Science **329**, 61 (2010).
[7] X.-L. Qi, T. L. Hughes, and S.-C. Zhang, Phys. Rev. B **78**, 195424 (2008).
[8] L. A. Wray, S.-Y. Xu, Y. Xia, D. Hsieh, A. V. Fedorov, Y. S. Hor, R. J. Cava, A. Bansil, H. Lin, and M. Z. Hasan, Nat. Phys. **7**, 32 (2011).
[9] Q. Liu, C.-X. Liu, C. Xu, X.-L. Qi, and S.-C. Zhang, Phys. Rev. Lett. **102**, 156603 (2009).

[10] D. West, Y. Y. Sun, S. B. Zhang, T. Zhang, X. Ma, P. Cheng, Y. Y. Zhang, X. Chen, J. F. Jia, and Q. K. Xue, Phys. Rev. B **85**, 081305 (2012).
[11] L. A. Wray, S.-Y. Xu, Y. Xia, D. Hsieh, A. V. Fedorov, Y. S. Hor, R. J. Cava, A. Bansil, H. Lin, and M. Z. Hasan, Nat. Phys. **7**, 32 (2011).
[12] M. R. Scholz, J. Sánchez-Barriga, D. Marchenko, A. Varykhalov, A. Volykhov, L. V. Yashina, and O. Rader, Phys. Rev. Lett. **108**, 256810 (2012).
[13] J. Honolka, A. A. Khajetoorians, V. Sessi, T. O. Wehling, S. Stepanow, J.-L. Mi, B. B. Iversen, T. Schlenk, J. Wiebe, N. B. Brookes, A. I. Lichtenstein, P. Hofmann, K. Kern, and R. Wiesendanger, Phys. Rev. Lett. **108**, 256811 (2012).
[14] J. S. Dyck, C. Drasar, P. Lostak, and C. Uher, Phys. Rev. B **71**, 115214 (2005).
[15] V. Kulbachinskii, A. Kaminskii, K. Kindo, Y. Narumi, K. Suga, P. Lostak, and P. Svanda, Physica (Amsterdam) **311B**, 292 (2002).
[16] Z. Zhou, Y.-J. Chien, and C. Uher, Appl. Phys. Lett. **87**, 112503 (2005).
[17] Y. R. Song, F. Yang, M.-Y. Yao, F. Zhu, L. Miao, J.-P. Xu, M.-X. Wang, H. Li, X. Yao, F. Ji, S. Qiao, Z. Sun, G. B. Zhang, B. Gao, C. Liu, D. Qian, C. L. Gao, and J.-F. Jia, Appl. Phys. Lett. **100**, 242403 (2012).
[18] Y. L. Chen, J.-H. Chu, J. G. Analytis, Z. K. Liu, K. Igarashi, H.-H. Kuo, X. L. Qi, S. K. Mo, R. G. Moore, D. H. Lu, M. Hashimoto, T. Sasagawa, S. C. Zhang, I. R. Fisher, Z. Hussain, and Z. X. Shen, Science **329**, 659 (2010).
[19] G. Rosenberg and M. Franz, Phys. Rev. B **85**, 195119 (2012).
[20] S.-Y. Xu, M. Neupane, C. Liu, D. Zhang, A. Richardella, L. Andrew Wray, N. Alidoust, M. Leandersson, T. Balasubramanian, J. Sanchez-Barriga, O. Rader, G. Landolt, B. Slomski, J. Hugo Dil, J. Osterwalder, T.-R. Chang, H.-T. Jeng, H. Lin, A. Bansil, N. Samarth, and M. Zahid Hasan, Nat. Phys. **8**, 616 (2012).
[21] D. Zhang, A. Richardella, D. W. Rench, S.-Y. Xu, A. Kandala, T. C. Flanagan, H. Beidenkopf, A. L. Yeats, B. B. Buckley, P. V. Klimov, D. D. Awschalom, A. Yazdani, P. Schiffer, M. Z. Hasan, and N. Samarth, Phys. Rev. B **86**, 205127 (2012).
[22] H. Li, Y. R. Song, M.-Y. Yao, F. Yang, L. Miao, F. Zhu, C. Liu, C. L. Gao, D. Qian, X. Yao, J.-F. Jia, Y. J. Shi, and D. Wu, Appl. Phys. Lett. **101**, 072406 (2012).
[23] A. Wachowiak, J. Wiebe, M. Bode, O. Pietzsch, M. Morgenstern, and R. Wiesendanger, Science **298**, 577 (2002).
[24] See Supplemental Material at http://link.aps.org/supplemental/10.1103/PhysRevLett.111.176802 for tests of tip polarization, zoomed-in hysteresis loops of Fig. 2 and definition of in (out of) plane polarization.
[25] R. Wiesendanger, Rev. Mod. Phys. **81**, 1495 (2009).
[26] Y. Jiang, Y. Wang, M. Chen, Z. Li, C. Song, K. He, L. Wang, X. Chen, X. Ma, and Q.-K. Xue, Phys. Rev. Lett. **108**, 016401 (2012).
[27] P. Cheng, C. Song, T. Zhang, Y. Zhang, Y. Wang, J.-F. Jia, J. Wang, Y. Wang, B.-F. Zhu, X. Chen, X. Ma, K. He, L. Wang, X. Dai, Z. Fang, X. Xie, X.-L. Qi, C.-X. Liu, S.-C. Zhang, and Q.-K. Xue, Phys. Rev. Lett. **105**, 076801 (2010).
[28] L. Fu, Phys. Rev. Lett. **103**, 266801 (2009).
[29] J. Henk, M. Flieger, I. V. Maznichenko, I. Mertig, A. Ernst, S. V. Eremeev, and E. V. Chulkov, Phys. Rev. Lett. **109**, 076801 (2012).
[30] C.-Z. Chang *et al.*, Science **340**, 167 (2013).
[31] H. Zhang, C. Liu, X. Qi, X. Dai, Z. Fang, and S. Zhang, Nat. Phys. **5**, 438 (2009).